Optical and Quantum Electronics 17 (1985) 1–14

Review
Matrix methods in treating decentred optical systems

WANG SHAOMIN
Department of Physics, Hangzhou University, Hangzhou, People's Republic of China

Received 29 November 1983

A set of matrix methods treating decentred optical systems in the paraxial approximation is reviewed. Misalignment phenomena of optical systems can generally be described by an augmented 4×4 matrix; propagation of optical rays in an asymmetric, inhomogeneous medium by a 3×3 matrix. In order to simplify the operations with these matrices, ray transfer flow graphs are introduced.

A lot of optical problems can be solved in a clear and simple manner, including optical arrays. Some examples are given.

1. Introduction

The 2×2 ray transfer matrices, introduced 18 years ago by Kogelnik and Li [1], are a useful instrument to describe the propagation of Gaussian beams through lens-like media or treating problems of optical resonators [2].

In recent years, remarkable progress in matrix optics has been achieved. Ray transfer matrices, describing Gaussian reflectivity (or transmission) [3–5], and the phase conjugate mirror have been introducted [6–8]. Moreover, the 2×2 matrix can be expanded to a 3×3 matrix applying to misaligned and asymmetric optical systems [9, 10].

A series of papers concerning this field has been published in China [11–24, 38–40]. The idea of this paper is to summarize the results so as to make them open to other scientists.

2. Expression of the 2×2 matrix

2.1. An augmented 4×4 matrix for misaligned systems

The ABCD law and the 2×2 matrices hold for centred systems only [1]. In reality, centred systems do not exist. An optical system is always slightly decentred or misaligned, due to tolerances of manufacturing or mechanical and thermal instabilities.

Let us start with a misaligned forward going system. In Fig. 1 r_1, r_1', r_2 and r_2' are ray parameters for the incoming and outgoing rays [1]; RP_1 and RP_2 mean the aligned reference planes, l is the geometrical distance from RP_1 to RP_2 and a, b, c and d denote the ray transfer matrix elements of this optical system. RP_{1m} and RP_{2m} mean the misaligned reference planes. ϵ and ϵ' express the misalignment parameters of this optical system, i.e. distance and slope between the misaligned axis and the ideal axis of this optical system at the input plane. The misaligned axis is defined by the straight line through the two centres of curvature as shown in Fig. 2a.

For the monocentric elements (Fig. 2b)

$$\epsilon/R + \epsilon' = \text{constant} \tag{1}$$

where R is the radius of surface curvature. Then ϵ or ϵ' can be taken as arbitrary, as long as the conditions of Equation 1 are fulfilled.

In view of the misaligned situation, we make a dual transformation of coordinates for studying the variations of the paraxial ray parameters, i.e.

0306–8919/85 $03.00 + .12

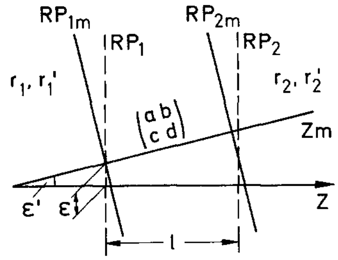

Figure 1 Misalignment diagram for a forward going system.

$$
\begin{array}{ccc}
r_1 & \xrightarrow{\text{The first coordinate transformation}} & r_{1\text{m}} \\
r_1' & & r_{1\text{m}}' \\
r_{1\text{m}} & \xrightarrow{\text{Coaxial propagation}} & r_{2\text{m}} \\
r_{1\text{m}}' & & r_{2\text{m}}' \\
r_{2\text{m}} & \xrightarrow{\text{The second coordinate transformation}} & r_2 \\
r_{2\text{m}}' & & r_2'
\end{array}
$$

which means that we take the aligned axis or ideal axis as a standard from beginning to end. According to the geometrical relation in Fig. 1, we obtain in paraxial approximation:

$$
\begin{bmatrix} r_2 \\ r_2' \end{bmatrix} = \begin{bmatrix} a & b \\ c & d \end{bmatrix} \begin{bmatrix} r_1 \\ r_1' \end{bmatrix} + \begin{bmatrix} \alpha & \beta \\ \gamma & \delta \end{bmatrix} \begin{bmatrix} \epsilon \\ \epsilon' \end{bmatrix} \tag{2}
$$

where α, β, γ and δ are called misalignment matrix elements determined by:

$$
\begin{aligned}
\alpha &= 1 - a \qquad & \beta &= l - b \\
\gamma &= -c \qquad & \delta &= 1 - d
\end{aligned} \tag{3}
$$

In order to represent Equation 2 as a matrix multiplication, both matrices can be compressed to a 4 x 4 matrix [11]:

$$
\begin{bmatrix} r_2 \\ r_2' \\ 1 \\ 1 \end{bmatrix} = \begin{bmatrix} a & b & \alpha\epsilon & \beta\epsilon' \\ c & d & \gamma\epsilon & \delta\epsilon' \\ 0 & 0 & 1 & 0 \\ 0 & 0 & 0 & 1 \end{bmatrix} \begin{bmatrix} r_1 \\ r_1' \\ 1 \\ 1 \end{bmatrix} \tag{4}
$$

The misalignment matrix for the backward going system is obtained by the substitutions:

$$
\delta = -1 - d \tag{5}
$$

As derived above, we notice that the augmented matrix holds for rays only. There is no augmented matrix for the equivalent transfer matrices [3–8].

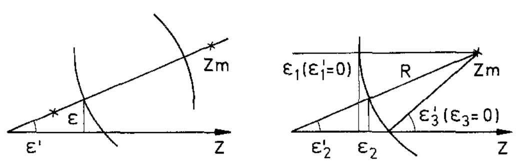

Figure 2 Definition of the misaligned axis: (a) general case, (b) monocentric elements.

If only a displacement is considered, the 4 x 4 matrix of Equation 4 will be reduced to a 3 x 3 matrix as follows:

$$\begin{bmatrix} r_2 \\ r_2' \\ 1 \end{bmatrix} = \begin{bmatrix} a & b & \alpha\epsilon \\ c & d & \gamma\epsilon \\ 0 & 0 & 1 \end{bmatrix} \begin{bmatrix} r_1 \\ r_1' \\ 1 \end{bmatrix} \tag{6}$$

with $\alpha = 1 - a$ and $\gamma = -c$, which is identical with that given in other works [9, 10].

2.2. An augmented 3 X 3 matrix for asymmetric systems

On the other hand, in practice, asymmetric inhomogeneous media are very often of interest. For example, the radial distribution of refractive index in a laser rod pumped asymmetrically or a self-focusing optical fibre made imperfectly. The index distribution may be written as:

$$n(r) = n(0)(1 + \alpha_0 r - \beta_0 r^2) \tag{7}$$

Here, α_0 denotes the asymmetric linear coefficient of the index. Using the differential equation describing ray propagation in inhomogeneous media [25]:

$$\frac{\mathrm{d}}{\mathrm{d}s}\left(n\frac{\mathrm{d}r}{\mathrm{d}s}\right) = \nabla n \tag{8}$$

in paraxial approximation, and using Equation 7, Equation 8 delivers:

$$\frac{\mathrm{d}^2 r}{\mathrm{d}z^2} + 2\beta_0 r - \alpha_0 = 0 \tag{9}$$

The solution of the inhomogeneous differential Equation 9 is:

$$\begin{aligned} r_2 &= \cos[l(2\beta_0)^{1/2}]r_1 + (2\beta_0)^{-1/2}\sin[l(2\beta_0)^{1/2}]r_1' + \frac{\alpha_0}{2\beta_0}\{1 - \cos[l(2\beta_0)^{1/2}]\} \\ r_2' &= -(2\beta_0)^{1/2}\sin[l(2\beta_0)^{1/2}]r_1 + \cos[l(2\beta_0)^{1/2}]r_1' + \alpha_0(2\beta_0)^{-1/2}\sin[l(2\beta_0)^{1/2}] \end{aligned} \tag{10}$$

where l is the length of this medium. Putting it into a square matrix form, we get [12]:

$$\begin{bmatrix} r_2 \\ r_2' \\ 1 \end{bmatrix} = \begin{bmatrix} a_0 & b_0 & e_0\alpha_0 \\ c_0 & d_0 & f_0\alpha_0 \\ 0 & 0 & 1 \end{bmatrix} \begin{bmatrix} r_1 \\ r_1' \\ 1 \end{bmatrix} \tag{11}$$

with:

$$\begin{aligned} a_0 &= \cos[l(2\beta_0)^{1/2}] \quad & b_0 &= (2\beta_0)^{-1/2}\sin[l(2\beta_0)^{1/2}] \quad & c_0 &= -(2\beta_0)^{1/2}\sin[l(2\beta_0)^{1/2}] \\ d_0 &= a_0 \quad & e_0 &= \frac{1}{2\beta_0}\{1 - \cos[l(2\beta_0)^{1/2}]\} \quad & f_0 &= (2\beta_0)^{-1/2}\sin[l(2\beta_0)^{1/2}] \end{aligned} \tag{12}$$

This is a canonical formalism of ray transfer matrices for an asymmetric inhomogeneous medium. If $\alpha_0 = 0$, it will be reduced to the well-known lens-like medium. If we use the transformation

$$r_0 = r - \alpha_0/2\beta_0 \tag{13}$$

Equation 9 becomes a homogeneous equation for r_0: $\mathrm{d}^2 r_0/\mathrm{d}z^2 + 2\beta_0 r_0 = 0$. The solution of this is identical with that of Equation 9. Then the physical meaning of the asymmetric phenomenon is becoming clear. It means that the asymmetric inhomogeneous medium is equivalent to a medium which is displaced radially by a distance $\alpha_0/2\beta_0$. Matrix 11 may thus be rewritten as Matrix 6:

$$\begin{bmatrix} r_2 \\ r_2' \\ 1 \end{bmatrix} = \begin{bmatrix} a_0 & b_0 & \alpha\epsilon \\ c_0 & d_0 & \gamma\epsilon \\ 0 & 0 & 1 \end{bmatrix} \begin{bmatrix} r_1 \\ r_1' \\ 1 \end{bmatrix} \tag{14}$$

with

$$\alpha = 1 - a_0 \quad \gamma = -c_0 \quad \epsilon = \alpha_0/2\beta_0 \tag{15}$$

Therefore the asymmetric inhomogeneous medium can be regarded as a special case of a misaligned system.

Why then did we derive the matrix in Equation 11? This is due to the fact that there are some special cases which cannot be described by the matrix in Equation 14. For example, when $\alpha_0 \neq 0, \beta_0 = 0$, i.e. there is an influence of the symmetric linear coefficient only, and a simplified form can be given by the matrix in Equation 11:

$$\begin{bmatrix} r_2 \\ r_2' \\ 1 \end{bmatrix} = \begin{bmatrix} 1 & l & \alpha_0 l^2/2 \\ 0 & 1 & \alpha_0 l \\ 0 & 0 & 1 \end{bmatrix} \begin{bmatrix} r_1 \\ r_1' \\ 1 \end{bmatrix} \tag{16}$$

2.3. Augmented matrices in reverse propagation

Now let us investigate ABCD matrix in reverse propagation. According to the definition of signs for ray parameters and the situation shown in Fig. 3, we get [13]:

$$\begin{bmatrix} a' & b' \\ c' & d' \end{bmatrix} = \begin{bmatrix} d & b \\ c & a \end{bmatrix} \frac{1}{\det|\mathrm{M}|} \tag{17}$$

When a paraxial ray through a centred optical system is reversed, a new ray transfer matrix is derived from the original one by interchanging elements a and d and dividing by the determinant of the matrix. If det $|\mathrm{M}| = 1$, Expression 17 will be reduced to the current expression, in which only the main diagonal elements are exchanged.

When the paraxial ray is passing through a misaligned optical system in reverse propagation, a reversed 4 x 4 matrix can be obtained as follows [26]:

$$\begin{bmatrix} a' & b' & \alpha'\epsilon & \beta'\epsilon' \\ c' & d' & \gamma'\epsilon & \delta'\epsilon' \\ \bigcirc & & 1 & 0 \\ & & 0 & 1 \end{bmatrix} = \begin{bmatrix} d & b & \delta\epsilon & (\delta l - \beta)\epsilon' \\ c & a & \gamma\epsilon & (\gamma l - \alpha)\epsilon' \\ \bigcirc & & 1 & 1 \\ & & 0 & 1 \end{bmatrix} \frac{1}{\det|\mathrm{M}|} \tag{18}$$

For the augmented 3 x 3 Matrix 11 then, we get:

$$\begin{bmatrix} a_0' & b_0' & e_0'\alpha_0 \\ c_0' & d_0' & f_0'\alpha_0 \\ 0 & 0 & 1 \end{bmatrix} = \begin{bmatrix} a_0 & b_0 & e_0\alpha_0 \\ c_0 & d_0 & f_0\alpha_0 \\ 0 & 0 & 1 \end{bmatrix} \tag{19}$$

The 3 x 3 matrix is unchanged when the paraxial ray is passing through an asymmetric inhomogeneous medium in reverse propagation, this is due to $a_0 = d_0$ and det $|\mathrm{M}| = 1$.

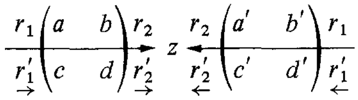

Figure 3 Transformation of ABCD matrix for forward and backward propagation.

2.4. Illustration with examples

For example, according to Fig. 2b and the matrix in Equation 4, Equations 3 and 5, the augmented 4 x 4 matrix of a misaligned spherical mirror, can be written as:

$$\begin{bmatrix} 1 & 0 & 0 & 0 \\ 2/R & 1 & -2\epsilon_1/R & 0 \\ \bigcirc & & 1 & 0 \\ & & 0 & 1 \end{bmatrix} \text{or} \begin{bmatrix} 1 & 0 & 0 & 0 \\ 2/R & 1 & -2\epsilon_2/R & -2\epsilon_2' \\ \bigcirc & & 1 & 0 \\ & & 0 & 1 \end{bmatrix} \text{or} \begin{bmatrix} 1 & 0 & 0 & 0 \\ 2/R & 1 & 0 & -2\epsilon_3' \\ \bigcirc & & 1 & 0 \\ & & 0 & 1 \end{bmatrix} \tag{20}$$

Which one is reasonable depends on the physical situation. And the augmented 4 x 4 matrix for misaligned phase-conjugate mirrors (PCM) [27] can be expressed by [14]:

$$M'_{\mathrm{PCMI}} = \begin{bmatrix} 1 & 0 & \bigcirc & \\ 0 & -1 & & \\ \bigcirc & & 1 & 0 \\ & & 0 & 1 \end{bmatrix} \tag{21}$$

which means that the PCM is a misalignment insensitive element. Some concrete formations of augumented 4 x 4 matrices for common optical elements and media are given in the Appendix.

It is well known that the PCM has the ability to compensate wavefront distortions, when the wavefront passes through an inhomogeneous medium there and back: a flat reflector

$$\begin{bmatrix} A & B \\ C & D \end{bmatrix} = \begin{bmatrix} d & b \\ c & a \end{bmatrix} \begin{bmatrix} 1 & 0 \\ 0 & 1 \end{bmatrix} \begin{bmatrix} a & b \\ c & d \end{bmatrix} = \begin{bmatrix} ad+bc & 2bd \\ 2ac & ad+bc \end{bmatrix} \tag{22}$$

cannot compensate the medium, characterized by *a, b, c, d*. But a PCM:

$$\begin{bmatrix} A & B \\ C & D \end{bmatrix} = \begin{bmatrix} d & b \\ c & a \end{bmatrix} \begin{bmatrix} 1 & 0 \\ 0 & -1 \end{bmatrix} \begin{bmatrix} a & b \\ c & d \end{bmatrix} = \begin{bmatrix} 1 & 0 \\ 0 & -1 \end{bmatrix} \tag{23}$$

will compensate the medium. If it is a misaligned optical element or system which can be described by 4 x 4 matrix, or an asymmetric inhomogeneous medium which can be described by 3 x 3 matrix, the wavefront passes through this element or system, there and back, the matrix reads [26]:

$$\begin{bmatrix} d & b & \delta\epsilon & (\delta l-\beta)\epsilon' \\ c & a & \gamma\epsilon & (\gamma l-\alpha)\epsilon' \\ \bigcirc & & 1 & 0 \\ & & 0 & 1 \end{bmatrix} \begin{bmatrix} 1 & 0 & \bigcirc & \\ 0 & -1 & & \\ \bigcirc & & 1 & 0 \\ & & 0 & 1 \end{bmatrix} \begin{bmatrix} a & b & \alpha\epsilon & \beta\epsilon' \\ c & d & \gamma\epsilon & \delta\epsilon' \\ \bigcirc & & 1 & 0 \\ & & 0 & 1 \end{bmatrix} = \begin{bmatrix} 1 & 0 & \bigcirc & \\ 0 & -1 & & \\ \bigcirc & & 1 & 0 \\ & & 0 & 1 \end{bmatrix} \tag{24}$$

or

$$\begin{bmatrix} a_0 & b_0 & e_0\alpha_0 \\ c_0 & d_0 & f_0\alpha_0 \\ 0 & 0 & 1 \end{bmatrix} \begin{bmatrix} 1 & 0 & 0 \\ 0 & -1 & 0 \\ 0 & 0 & 1 \end{bmatrix} \begin{bmatrix} a_0 & b_0 & e_0\alpha_0 \\ c_0 & d_0 & f_0\alpha_0 \\ 0 & 0 & 1 \end{bmatrix} = \begin{bmatrix} 1 & 0 & 0 \\ 0 & -1 & 0 \\ 0 & 0 & 1 \end{bmatrix} \tag{25}$$

it is clear that the PCM has the ability to compensate distortions even in misaligned systems.

On the basis of the augmented 4 x 4 matrices and 3 x 3 matrices a lot of practical problems have been solved, e.g. laser alignment by the three-point method in a vacuum line has been successfully applied to the measurement of dam deformation [15, 16]. Compared with other laser methods, it has

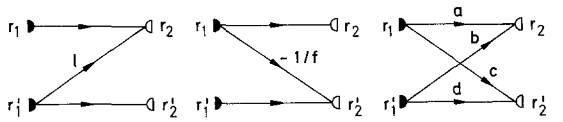

Figure 4 Ray transfer flow graphs for the most fundamental systems: (a) uniform medium, (b) thin lens, (c) arbitrary optical system.

some advantages: the horizontal and vertical deflections can be measured at the same time, raising accuracy about 10 times and raising work efficiency approximately 20 times.

According to the definition of misalignment sensitivity of resonators [28], the misalignment sensitivity of multi-element spherical resonators [17], corner-cube resonators [18], phase-conjugate resonators (PCR) [14] and additional loss of the solid-state laser caused by asymmetric pump [19] have been obtained. The eikonal function, diffraction integral and some other problems in physical optics for the decentred systems have been given as well [20].

However, the multiplication algebras of 4 x 4 matrix and 3 x 3 matrix are rather complicated. In order to simplify these operations the ray transfer flow graphs will be discussed in the next section.

3. Flow graph instead of transfer matrix

3.1. Ray transfer flow graph

The flow graph algebra is a kind of graph theory. Flow graphs are graphical languages for linear equations. They are topological structures consisting of points and lines. The points in a graph represent variables, and the lines connecting points indicate the relations among these points.

How do we form a flow graph? At first, we have to give the formation of causality of these equations. Fortunately, the ray transfer matrix arises from a causality of linear equations, so we can use the ray transfer matrix directly to obtain its corresponding flow graph. For example, the ray transfer flow graphs for uniform medium, thin lens and arbitrary optical systems are shown in Fig. 4 [21], in which, if the line is not labelled by a matrix element, it means the matrix element is equal to unity. For the misaligned optical systems, the 4 x 4 matrix, Equation 4, is represented by the graph shown in Fig. 5.

The augmented 3 x 3 matrix of Equation 11 can also be expressed by a ray transfer flow graph. In Fig. 6 the asymmetric effect is shown. Some concrete ray transfer flow graphs for misaligned elements and media are given in the Appendix.

When a flow graph has been formed we can apply Mason's rule [29] to obtain the solutions. For the cascade graph, Mason's rule reduces to a simple expression. In particular, when we are only interested in one of the output variables subject to one of the input variables, it will be simplified to:

$$Y_j = X_i \sum_{k=1}^{K} P_k \tag{26}$$

where Y_j is one of the output variables, X_i is one of the input variables; P_k means the product of the matrix elements along the path k, and K denotes every possible path.

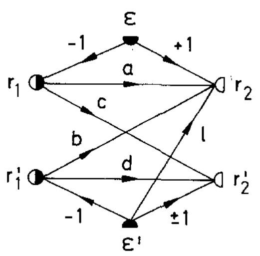

Figure 5 Topological structure of ray transfer flow graph for misaligned systems.

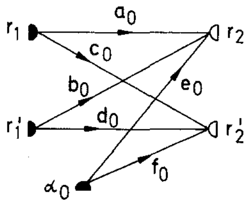

Figure 6 Corresponding ray transfer flow graph for 3 X 3 matrix.

3.2. Examples

There are two kinds of telescopes: external focusing and internal focusing, as shown on the left of Fig. 7. If the telescope parameters and the manufacturing tolerances of ϵ and ϵ' are the same for both, let us investigate the focusing errors (r_2 and r'_2 affected by ϵ and ϵ').

If we consider only the output parameters subject to the tolerances, the complicated multiplication of 4 x 4 matrix will be avoided, and the solutions can be obtained by means of the simplified form of Mason's rule [26] as shown on the right of Fig. 7. It reveals that the internal focusing telescope is less sensitive to misalignment than the external focusing one.

As discussed above, in view of the msialignment phenomena of optical systems, an augmented 4 x 4 matrix instead of 2 x 2 matrix has been introduced. In consideration of the propagation of optical rays in an asymmetric, inhomogeneous medium, an augmented 3 x 3 matrix instead of 2 x 2 matrix has been introduced as well, and in order to simplify the operations the ray transfer flow graphs have been used. These graphs allow a series of difficult decentred problems to be solved [11, 12, 21, 26]. However, the basis of these methods is the 4 x 4 matrix which will be applied to solve an interesting problem in the next section.

4. Augmented matrix in treating arrays

4.1. Non-Gaussian imaging properties of arrays

Some experiments have demonstrated that corner-cube arrays can be used to approximate phase conjugation [30–33]. To compare the corner-cube arrays with conventional adaptive optics (COAT) [34, 35], we note that the arrays offer the advantages of unlimited dynamic range, much higher response speed, lower weight, lower cost and simplicity. The arrays also have significant potential advantages in respect of nonlinear phase conjugation: they are passive elements, the return frequency is always equal to the input frequency, they have larger areas and arbitrarily weak signals can be conjugated. The corner-cube arrays are the well-known plastic retro reflectors used on bicycles and highway signs.

On the other hand, the non-Gaussian imaging properties of GRIN fibre arrays were discovered in 1982 [36].

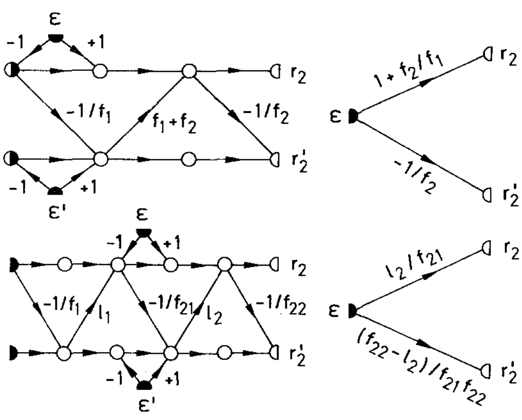

Figure 7 Focusing errors of telescopes: (a) external focusing, (b) internal focusing.

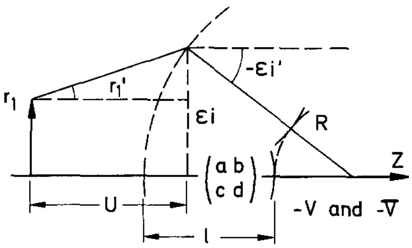

Figure 8 An optical element array.

By optical element arrays we mean the radial combination of optical elements. Each element must be small enough that the incident wave can be approximated by a plane wave across its aperture, but large enough to give negligible diffraction. Therefore, there are problems in geometrical optics. However, it is difficult to analyse the imaging properties of optical element arrays by means of classical geometrical optics because they are beyond the Gaussian approximation. Therefore, the corner-cube arrays were called pseudo-conjugators [37].

In fact, the arrangement of an individual optical element of array can be regarded as a misalignment element, shown in Fig. 8. The regular misalignment in paraxial region can be expressed as follows:

$$\epsilon_i = r_1 + u r_1' \tag{27}$$

$$\epsilon_i' = -\epsilon_i / R \tag{28}$$

The ray transfer matrix relating object plane and image plane can be written as:

$$\begin{bmatrix} A & B & E & F \\ C & D & G & H \\ 0 & 0 & 1 & 0 \\ 0 & 0 & 0 & 1 \end{bmatrix} = \begin{bmatrix} 1 & -V & 0 & 0 \\ 0 & 1 & 0 & 0 \\ 0 & 0 & 1 & 0 \\ 0 & 0 & 0 & 1 \end{bmatrix} \begin{bmatrix} a & b & \alpha\epsilon_i & \beta\epsilon_i' \\ c & d & \gamma\epsilon_i & \delta\epsilon_i' \\ 0 & 0 & 1 & 0 \\ 0 & 0 & 0 & 1 \end{bmatrix} \begin{bmatrix} 1 & u & 0 & 0 \\ 0 & 1 & 0 & 0 \\ 0 & 0 & 1 & 0 \\ 0 & 0 & 0 & 1 \end{bmatrix}$$

$$= \begin{bmatrix} a - cV & au + b - V(cu + d) & (\alpha - \gamma V)\epsilon_i & (\beta - \delta V)\epsilon_i' \\ c & cu + d & \gamma\epsilon_i & \delta\epsilon_i' \\ 0 & 0 & 1 & 0 \\ 0 & 0 & 0 & 1 \end{bmatrix} \tag{29}$$

In view of the regularity of the misalignment, substituting Equations 27 and 28 into the 4 x 4 matrix of Equation 29, gives a 2 x 2 matrix [22].

$$\begin{bmatrix} \underline{r_2} \\ \underline{r_2'} \end{bmatrix} = \begin{bmatrix} (a - c\bar{V}) + [(\alpha - \gamma\bar{V}) - (\beta - \delta\bar{V})/R] & [aU + b - \bar{V}(cU + d)] + U[(\alpha - \gamma\bar{V}) - (\beta - \delta\bar{V})/R] \\ c + (\gamma - \delta/R) & (cU + d) + U(\gamma - \delta/R) \end{bmatrix}$$

$$\times \begin{bmatrix} r_1 \\ r_1' \end{bmatrix} = \begin{bmatrix} \underline{A} & \underline{B} \\ \underline{C} & \underline{D} \end{bmatrix} \begin{bmatrix} r_1 \\ r_1' \end{bmatrix} \tag{30}$$

It is a synthetical imaging matrix for an optical element array. All of the first order synthetical imaging properties are embedded in this matrix, in which the synthetical image distance has been written as $-\bar{V}$ to distinguish it from the individual image distance $-V$.

An image is formed if all rays coming from a point in the object space go through one point in the image space. The relation between these two conjugate distances follows from the top right hand element, which vanishes in the imaging matrix:

$$\bar{V} = \frac{[(R+b-l)/R]U+b}{[(d\mp 1)/R]U+d} \tag{31}$$

Where $-$ is applied to the forward going arrays, and $+$ is appied to the backward going arrays. Evidently the image plane for best synthetical focus will not coincide with the image plane of best focus for the individual element, which is subject to the ABCD law. Therefore, the synthetical image is not a Gaussian image. The angular magnification, transverse magnification, axial magnification, focal power, focal planes, principal planes and nodal points of the synthetical image for the arrays can also be obtained by means of the imaging matrix elements $\underline{A}$, $\underline{B}$, $\underline{C}$ and $\underline{D}$.

It is convenient to introduce a ray transfer matrix for arrays to describe the synthetical image object transformation. Comparing Equation 31 with the ABCD law, we find:

$$\begin{bmatrix} \underline{a_1} & \underline{b_1} \\ \underline{c_1} & \underline{d_1} \end{bmatrix} = \begin{bmatrix} (R+b-l)/R & b \\ (d\mp 1)/R & d \end{bmatrix} \tag{32}$$

with

$$\det|\mathrm{M}_1| = (dR \pm b - dl)/R \tag{33}$$

If we would like to know the physical meaning of the transformation for an optical system, or if we want to calculate some problems in a simple way, this can be done by transforming the ray transfer matrix through the ABCD law to form an equivalent transfer matrix. For example, an arbitrary optical element may be regarded as a thin lens (with variable parameters) if this element can be described by a ray transfer matrix, i.e.:

$$q_2 = \frac{a_1\hat{q}_1+b_1}{c_1\hat{q}_1+d_1} = \frac{q_1}{\left(\dfrac{c_1\hat{q}_1+d_1}{a_1\hat{q}_1+b_1}-\dfrac{1}{q_1}\right)q_1+1} = \frac{a_2q_1+b_2}{c_2q_1+d_2} \tag{34}$$

According to this concept, an equivalent transfer matrix for arrays can be given:

$$\begin{bmatrix} \underline{a_2} & \underline{b_2} \\ \underline{c_2} & \underline{d_2} \end{bmatrix} = \begin{bmatrix} 1 & 0 \\ \dfrac{\underline{c_1}U+\underline{d_1}}{\underline{a_1}U+\underline{b_1}}-\dfrac{1}{U} & 1 \end{bmatrix} = \begin{bmatrix} 1 & 0 \\ \dfrac{(d\mp l)/R}{\left(\dfrac{R+b-l}{R}+\dfrac{b}{U}\right)}+\left\{\dfrac{d}{\left(\dfrac{R+b-l}{R}+\dfrac{b}{U}\right)}-1\right\} & 1 \end{bmatrix} \tag{35}$$

with

$$\det|\mathrm{M}_2| = 1 \tag{36}$$

For a plane array ($R=\infty$), Equation 31, and the matrices in Equations 32 and 35 reduce to:

$$\bar{V} = (U+b)/d$$

$$\begin{bmatrix} \underline{a_1} & \underline{b_1} \\ \underline{c_1} & \underline{d_1} \end{bmatrix} = \begin{bmatrix} 1 & b \\ 0 & d \end{bmatrix} \text{ and } \begin{bmatrix} \underline{a_2} & \underline{b_2} \\ \underline{c_2} & \underline{d_2} \end{bmatrix} = \begin{bmatrix} 1 & 0 \\ \dfrac{d}{U+b}-\dfrac{1}{U} & 1 \end{bmatrix} \tag{37}$$

If we select optical elements with $b=0$ and $d=-1$ to form an array, Equation 37 will be simplified further:

$$\bar{V} = -U$$

$$\begin{bmatrix} \underline{a_1} & \underline{b_1} \\ \underline{c_1} & \underline{d_1} \end{bmatrix} = \begin{bmatrix} 1 & 0 \\ 0 & -1 \end{bmatrix} \text{ and } \begin{bmatrix} \underline{a_2} & \underline{b_2} \\ \underline{c_2} & \underline{d_2} \end{bmatrix} = \begin{bmatrix} 1 & 0 \\ -2/U & 1 \end{bmatrix} \tag{38}$$

They are identical with that of PCM formed by DFWM [6–8, 27]. That is why the corner-cube arrays have phase conjugate properties or non-Gaussian imaging properties.

4.2. Some new types of PCM formed by arrays

As discussed above, phase conjugation is equivalent to imaging with equal distances of object and image. This is a characteristic of phase conjugation in geometrical optics. We can find a series of arrays, which may perform phase conjugation if one compares this condition with Equation 31. An array consists of reflection elements with:

$$l = 0 \quad \text{and} \quad R = -U \tag{39}$$

its conjugate distance, Equation 31, will be simplified correspondingly. It is a phase conjugate principle of COAT. However, COAT is controlled by means of pistons, so the distortions cannot be completely compensated and the structures are rather complicated.

Let us take simple, practical and fixed plane arrays ($R = \infty$), as long as we select optical elements with:

$$b = 0 \qquad d = -1 \tag{40}$$

to form arrays, then the conjugate distance, Equation 31, is also reduced to Equation 38. It is a basic condition for arrays as phase conjugators, including corner-cube arrays. However, the ray transfer matrix elements depend on the way we select the reference planes of optical elements. We can apply the moving reference plane technique to find more optical elements of which the arrays may perform phase conjugation [22, 26]. A generalized condition for arrays as phase conjugators can be expressed as follows:

$$a = d, \quad \text{with} \quad b^+ = -(1+d)/c \quad \text{or} \quad b^+ = b/(1-a) \tag{41}$$

where b^+ means the shift of the reference planes.

According to this principle a lot of new types of PCM formed by arrays have been demonstrated, e.g. GRIN fibre array [38], an unusual thick lens array [39] and a bead array [23]. A sketch of the bead array is shown in Fig. 9. The ray transfer matrix of an individual optical element for RP reads:

$$\begin{bmatrix} a & b \\ c & d \end{bmatrix} = \begin{bmatrix} \dfrac{n-4}{n} & \dfrac{-4R_0}{n} \\ \dfrac{-2(2-n)}{nR_0} & \dfrac{n-4}{n} \end{bmatrix} \tag{42}$$

which satisfies Equation 41. Taking $b^+ = -R$, we get a new ray transfer matrix for RP^* as follows:

$$\begin{bmatrix} a^* & b^* \\ c^* & d^* \end{bmatrix} = \begin{bmatrix} -1 & 0 \\ \dfrac{-2(2-n)}{nR_0} & -1 \end{bmatrix} \tag{43}$$

Substituting these matrix elements into Equation 31 and using the matrices in Equations 32–35, the resulting expressions are identical with those of the corner-cube array (Equation 38). The ability to compensate distortions is shown in Fig. 10.

However, notice that the ray transfer matrix for a bead with c^* or c (Equation 43) is not identical with that of the corner-cube, which is related to synthetical imaging aberrations.

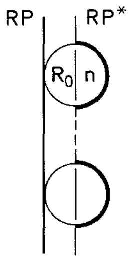

Figure 9 A bead array.

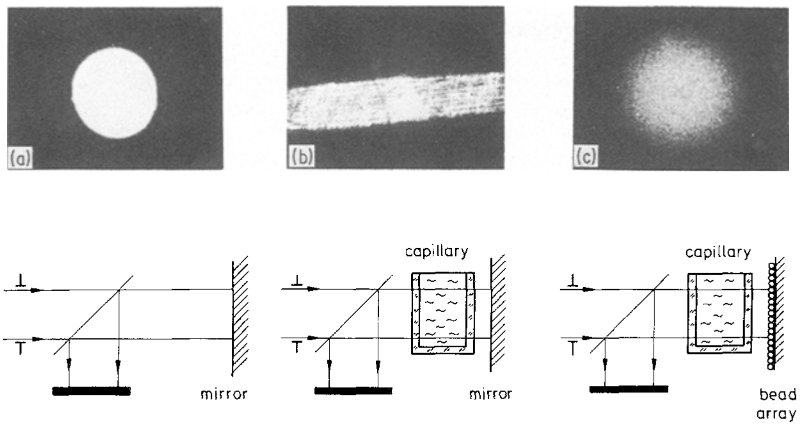

Figure 10 Ability to compensate distortions for a bead array: (a) ordinary mirror without distortions, (b) ordinary mirror with distortions, (c) a bead array with distortions.

4.3. Synthetical imaging aberrations for arrays

Up to now the individual element sizes (σ) have been neglected, but in order to analyse the synthetical imaging aberrations, the individual element sizes must be taken into account. Therefore Equation 27 may be rewritten as:

$$\epsilon_i = r_1 + Ur'_{i10} = r_1 + U(r'_{i1} \mp \sigma_i/U) \tag{44}$$

with

$$\sigma_i = \sigma(1 - \epsilon_i'^2)^{1/2} \tag{45}$$

where r'_{i10} is the slope between the axis of array and the ray coming from the object and ending on the centre of the individual elements. According to the matrix in Equation 29, the geometrical parameters of rays for an image-forming element i at the synthetic image surface can be written as:

$$\begin{bmatrix} \underline{r}_{i2} \\ \underline{r}'_{i2} \\ 1 \\ 1 \end{bmatrix} = \begin{bmatrix} a - c\bar{V} & aU + b - \bar{V}(cU + d) & (\alpha - \gamma\bar{V})\epsilon_i & (\beta - \delta\bar{V})\epsilon'_i \\ c & cU + d & \gamma\epsilon_i & \delta\epsilon'_i \\ & & 1 & 0 \\ & & 0 & 1 \end{bmatrix} \begin{bmatrix} r_1 \\ r'_{i1} \\ 1 \\ 1 \end{bmatrix} \tag{46}$$

From Equations 28, 44 and 46 follows:

$$\underline{r}_{i2} = \underline{A}r_1 + \underline{B}r'_{i10} \pm \sigma_i[(aU + b) - \bar{V}(cU + d)]/U \tag{47}$$

Then the synthetical imaging aberrations are obtained [24]:

$$\Delta\underline{r}_{i2} = \underline{r}_{i20} - \underline{r}_{i2} = \mp\sigma(1 - \epsilon_i'^2)^{1/2}\left\{(aU + b) - \left[\left(\frac{R + b - l}{R}\right)U + b\right](cU + d)\Big/\left[\left(\frac{d \mp 1}{R}\right)U + d\right]\right\}\Big/U \tag{48}$$

Substituting Equation 28 into the matrices in Equations 29 and 46, we find that the synthetical image surface coincides with the individual image surface, and the synthetical imaging aberrations are eliminated if the following condition is satisfied:

$$\bar{V} = \frac{\alpha R - \beta}{\gamma R - \delta} = V \tag{49}$$

which may be called the $\alpha\beta\gamma\delta$ condition.

For the phase conjugators formed by plane arrays, the synthetical imaging aberrations (Equation 48) can be simplified to:

$$\Delta\underline{r}_2 = \mp\sigma(cU - 2) \tag{50}$$

The imaging qualities or phase conjugate properties of arrays with c or c^* are better than that of $c = 0$ or $c^* = 0$, in some cases.

4.4. Main characteristic of compound eye

As discussed in Section 2.3, the ray transfer matrix in reverse propagation can be completely expressed by interchanging matrix elements *a* and *d* and dividing by the determinant of this matrix. Therefore, the reversed transfer matrix for arrays may be written as:

$$\begin{bmatrix} a_1' & b_1' \\ c_1' & d_1' \end{bmatrix} = \begin{bmatrix} d & b \\ (d \mp 1)/R & (R+b-l)/R \end{bmatrix} \Bigg/ \frac{dR \pm b - dl}{R} \tag{51}$$

We are interested in:

$$\det |\mathrm{M}_1| = (dR \pm b - dl)/R = 0 \tag{52}$$

It is an irreducible matrix; we cannot find any reversed matrix in this case. If the radius of curvature for arrays is selected as:

$$R = (dl \mp b)/d \tag{53}$$

then a novel result is produced:

$$\bar{V} = b/d \tag{54}$$

which means that all objects in the object space will be imaged at an identical plane, which may be a characteristic of the compound inset eye. At least it is possible to design a lens formed by arrays for which the depth of field approaches infinity [40].

All of the results in this section are based on the augmented 4 x 4 matrix of Equation 4.

Acknowledgement

The author is grateful to Professor Dr H. Weber for his valuable discussions.

Appendix

Augmented ray transfer matrices and their corresponding flow graphs for some misaligned elements and media.

Number	Description	Misaligned diagram	Augmented 4 X 4 ray transfer matrix	Corresponding flow graph
1	Misaligned uniform medium	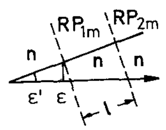	$\begin{bmatrix} 1 & l & \bigcirc & \\ 0 & 1 & & \\ \bigcirc & & 1 & 0 \\ & & 0 & 1 \end{bmatrix}$	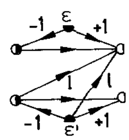
2	Misaligned spherical interface*	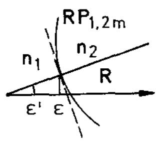	$\begin{bmatrix} 1 & 0 & 0 & 0 \\ c_1 & n_1/n_2 & -\epsilon c_1 & \epsilon'(1-n_1/n_2) \\ \bigcirc & & 1 & 0 \\ & & 0 & 1 \end{bmatrix}$	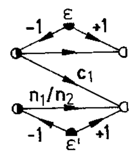
3	Misaligned plane interface	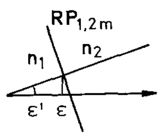	$\begin{bmatrix} 1 & 0 & 0 & 0 \\ 0 & n_1/n_2 & 0 & \epsilon'(1-n_1/n_2) \\ \bigcirc & & 1 & 0 \\ & & 0 & 1 \end{bmatrix}$	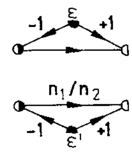
4	Misaligned planoparallel	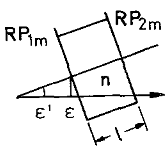	$\begin{bmatrix} 1 & l/n & 0 & \epsilon'(1-1/n)l \\ 0 & 1 & 0 & 0 \\ \bigcirc & & 1 & 0 \\ & & 0 & 1 \end{bmatrix}$	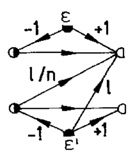

TABLE (contd.)

Number	Description	Misaligned diagram	Augmented 4 × 4 ray transfer matrix	Corresponding flow graph
5	Misaligned thick lens†	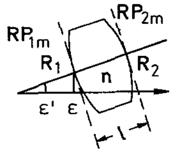	$\begin{bmatrix} a_2 & b_2 & \alpha_2\epsilon & \beta_2\epsilon' \\ c_2 & d_2 & \gamma_2\epsilon & \delta_2\epsilon' \\ \multicolumn{2}{c}{\bigcirc} & 1 & 0 \\ & & 0 & 1 \end{bmatrix}$	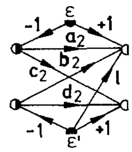
6	Misaligned thin lens	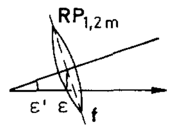	$\begin{bmatrix} 1 & 0 & 0 & 0 \\ -1/f & 1 & \epsilon/f & 0 \\ \multicolumn{2}{c}{\bigcirc} & 1 & 0 \\ & & 0 & 1 \end{bmatrix}$	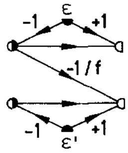
7	Misaligned wedge	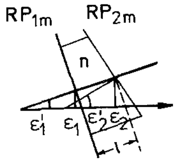	$\begin{bmatrix} 1 & l/n & 0 & (1-1/n)l\epsilon_1' \\ 0 & 1 & 0 & (1-n)(\epsilon_2'-\epsilon_1') \\ \multicolumn{2}{c}{\bigcirc} & 1 & 0 \\ & & 0 & 1 \end{bmatrix}$	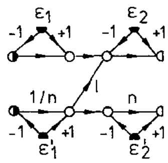
8	Misaligned lens-like medium‡	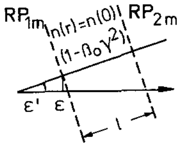	$\begin{bmatrix} a_0 & b_0 & \alpha_0\epsilon & \beta_0\epsilon' \\ c_0 & d_0 & \gamma_0\epsilon & \delta_0\epsilon' \\ \multicolumn{2}{c}{\bigcirc} & 1 & 0 \\ & & 0 & 1 \end{bmatrix}$	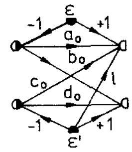
9	Misaligned spherical mirror	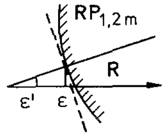	$\begin{bmatrix} 1 & 0 & 0 & 0 \\ 2/R & 1 & -2\epsilon/R & -2\epsilon' \\ \multicolumn{2}{c}{\bigcirc} & 1 & 0 \\ & & 0 & 1 \end{bmatrix}$	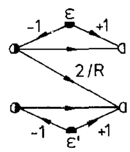
10	Misaligned flat mirror	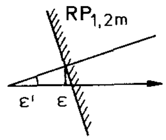	$\begin{bmatrix} 1 & 0 & 0 & 0 \\ 0 & 1 & 0 & -2\epsilon' \\ \multicolumn{2}{c}{\bigcirc} & 1 & 0 \\ & & 0 & 1 \end{bmatrix}$	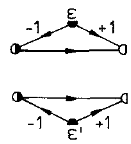
11	Misaligned corner-cube reflector	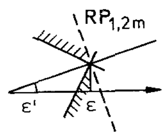	$\begin{bmatrix} -1 & 0 & 2\epsilon & 0 \\ 0 & -1 & 0 & 0 \\ \multicolumn{2}{c}{\bigcirc} & 1 & 0 \\ & & 0 & 1 \end{bmatrix}$	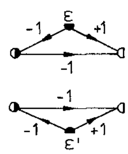
12	Misaligned PCM formed by DFWM	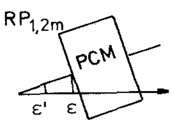	$\begin{bmatrix} 1 & 0 & \multicolumn{2}{c}{\bigcirc} \\ 0 & -1 & & \\ \multicolumn{2}{c}{\bigcirc} & 1 & 0 \\ & & 0 & 1 \end{bmatrix}$	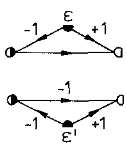

$^*c_1 = -(1-n_1/n_2)/R$

$^\dagger a_2 = 1-(1-1/n)l/R_1,\ b_2 = l/n,\ c_2 = -\left[(n-1)\left(\dfrac{1}{R_1}+\dfrac{1}{R_2}\right)-(n-1)^2 l/nR_1R_2\right],\ d_2 = 1-(1-1/n)l/R_2$

$^\ddagger\beta_0 > 0{:}\ a_0 = \cos[l(2\beta_0)^{1/2}],\ b_0 = \dfrac{1}{2\beta_0}\sin[l(2\beta_0)^{1/2}],\ c_0 = -2\beta_0 b_0,\ d_0 = a_0$

$\beta_0 < 0{:}\ a_0 = \cosh[l(-2\beta_0)^{1/2}],\ b_0 = \dfrac{1}{(-2\beta_0)^{1/2}}\sinh[l(-2\beta_0)^{1/2}],\ c_0 = -2\beta_0 b_0,\ d_0 = a_0$

References

1. H. KOGELNIK and T. LI, *Appl. Opt.* **5** (1966) 1550.
2. A. YARIV, 'Quantum Electronics' (Holt, Rinehart and Winston, New York, 1975).
3. A. YARIV and P. YEH, *Opt. Commun.* **13** (1975) 370.
4. U. GANIEL and A. HARDY, *Appl. Opt.* **15** (1976) 2145.
5. A. YARIV, 'Introduction to Optical Electronics' (Holt, Rinehart and Winston, New York, 1976).
6. W. SHAOMIN and H. WEBER, *Opt. Commun.* **41** (1982) 360.
7. W. SHAOMIN, H. XICHUN and Y. JUN, *Acta Opt. Sinica* **3** (1983) 41 (in Chinese).
8. W. SHAOMIN and H. WEBER, 'Fundamental Modes of Stimulated Scattering Phase-Conjugate Resonators' (to be published).
9. A. GERRARD and J. M. BURCH, 'Introduction to Matrix Methods in Optics' (John Wiley and Sons, New York, 1975).
10. J. A. ARNAUD, 'Beam and Fibre Optics' (Academic Press, New York, 1976).
11. W. SHAOMIN, *J. Hangzhou University* **3** (1979) 42 (in Chinese).
12. *Idem, Sci. Sinica* **25** (1982) 72.
13. *Idem, Appl. Laser* **2** (1983) 13 (in Chinese).
14. *Idem, Kexue Tongabao* **28** (1983) 173.
15. W. SHAOMIN, W. SHIAOJING, Y. CHENGRENG, C. ZULI, Z. JINGMIN and J. JIYI, *Laser J.* **3** (1980) 54 (in Chinese).
16. X. CHANG and W. SHAOMIN, *Sci. Sinica*, in press.
17. W. SHAOMIN, *Nature* **4** (1981) 236 (in Chinese).
18. H. WEIGANG, H. XICHUN and W. SHAOMIN, *Chin. J. Lasers* **10** (1983) 58 (in Chinese).
19. W. SHAOMIN and W. SIAOJING, *J. Hangzhou University* **9** (1982) 168 (in Chinese).
20. H. XICHUN, H. WEIGANG and W. SHAOMIN, *Acta Phys. Sinica* **31** (1982) 1655 (in Chinese).
21. W. SHAOMIN, *Laser J.* **2** (1979) 1 (in Chinese).
22. *Idem, J. Hangzhou University* **10** (1983) 477 (in Chinese).
23. H. WEISHAI, J. XIUMING, C. YINGLY, Z. JIAJU, Z. JINMIN and W. SHAOMIN, *Chin. J. Laser* **10** (1983) 191 (in Chinese).
24. W. SHAOMIN, 'Non-gaussian imaging properties and synthetical imaging qualities of optical element arrays', Topical meeting on Gradient-index optical imaging systems, US, May, 1984.
25. M. BORN and E. WOLF, 'Principles of Optics' (Pergamon Press, Oxford, 1980).
26. W. SHAOMIN and H. WEBER, 'Matrix Optics' (Physica-Verlag, in press).
27. A. YEUNG, J. D. FEKETE, D. M. PEPPER and A. YARIV, *IEEE* **QE-15** (1979) 1180.
28. R. HAUCK, H. P. HORTZ and H. WEBER, *Appl. Opt.* **19** (1980) 598.
29. E. J. HENLEY and R. A. WILLIAMS, 'Graphs Theory in Modern Engineering' (Academic Press, New York, 1973).
30. V. K. ORLOV, Ya. Z. VIRNIK, S. P. VOROTILIN, V. B. GERASIMOV, Yu. A. KALININ and A. Ya. SAGALOVICH, *Sov. J. Quantum Electr.* 8 (1978) 799.
31. H. H. BARRETT and S. F. JACOBS, *Opt. Lett.* **4** (1979) 190.
32. P. MATHIEU and P. A. BELANGER, *Appl. Opt.* **19** (1980) 2262.
33. S. F. JACOBS, *Opt. Eng.* **21** (1982) 281.
34. R. H. FREEMAN, R. J. FREIBERG and H. R. GARCIA, *Opt. Lett.* **2** (1978) 61.
35. T. SATO, Y. NAGURA, O. IKEDA and T. HATSUZAWA, *Appl. Opt.* **21** (1982) 1778.
36. J. D. REES, *Appl. Opt.* **21** (1982) 1009.
37. T. R. O'MEARA, *Opt. Eng.* **21** (1982) 271.
38. W. SHAOMIN, Z. GUOSHENG, W. MEIYING, P. LIANHUI and T. LIJUAN, *Acta Phys. Sinica* **32** (1983) 1957 (in Chinese).
39. W. SHAOMIN, Z. JINMIN, W. SHIAOJING, Y. CHENGRENG and Z. ZEXAN, *Appl. Laser* 5 (1983) 27 (in Chinese).
40. W. SHAOMIN, Y. CHENGREN, T. WEIZIANG and Z. ZEXAN, An optical element formed by array whose Det = 0 and its potential applications, ICO-13, Japan, August 1984.